



The Terminal Tracking Camera System on the NASA *Lucy* Trojan Asteroid Discovery Mission

J.F. Bell III¹ · Y. Zhao¹ · E. Cisneros¹ · M. Beasley² · C. Olkin² · M.A. Caplinger³ · M.A. Ravine³ · J.A. Schaffner³ · M.J. Clark³ · J. Shamah³ · P. Faiks⁴ · S. Mottola⁵ · C. Adam⁶ · E. Lessac-Chenen⁶ · B.J. Bos⁷

Received: 17 June 2023 / Accepted: 21 November 2023 / Published online: 13 December 2023
© The Author(s) 2023

Abstract

The Terminal Tracking Camera system (TTCam) on the NASA *Lucy* Trojan asteroid Discovery mission consists of a pair of block redundant cameras and their associated electronics that are mounted on the spacecraft's Instrument Pointing Platform and co-boresighted with the rest of the mission's science payload instruments. The primary function of the TTCams is as a navigation system designed to provide an autonomous onboard late pre-encounter update of the location of each asteroid flyby target relative to the spacecraft. However, once the terminal tracking function is complete, the TTCam system will also provide $11.0^\circ \times 8.2^\circ$ field of view broadband (425–675 nm) images during the close approach phase of each asteroid flyby that will be used for scientific analyses like shape modeling and assessment of each target's geology and topography. This paper provides an overview of the TTCam cameras and electronics, the science-focused requirements that the system is designed to meet, pointers to pre-flight calibration and in-flight calibration details for the cameras, as well as a high-level summary of the kinds of science that these images will enable for the mission.

Keywords NASA *Lucy* mission · Trojan asteroids · Spacecraft instrumentation · Deep space cameras

1 Introduction

The *Lucy* mission was chosen for flight in 2017 as part of NASA's Discovery Program of low-cost, competitively selected deep space robotic science missions. The mission was suc-

✉ J.F. Bell III
Jim.Bell@asu.edu

¹ School of Earth and Space Exploration, Arizona State University, Tempe AZ, USA

² Southwest Research Institute, Boulder, CO, USA

³ Malin Space Science Systems, Inc., San Diego CA, USA

⁴ Lockheed Martin Space, Littleton, CO, USA

⁵ German Aerospace Center (DLR), Berlin, Germany

⁶ KinetX Inc., Tempe, AZ, USA

⁷ NASA Goddard Spaceflight Center, Greenbelt, MD, USA

cessfully launched on October 16, 2021 and conducted its first Earth Gravity Assist (EGA) flyby on October 16, 2022. After a flyby of main belt asteroids (152830) Dinkinesh in 2023 and (52246) Donaldjohanson in 2025, *Lucy* will conduct five flyby encounters of eight members of Jupiter's Trojan asteroid population between 2027 and 2033. The primary goals of the *Lucy* mission include assessing the diversity of the Trojan asteroids, determining their surface composition, assessing their geology, determining their bulk properties (including mass and density), and searching for satellites and rings. Additional details about the science goals of the *Lucy* mission can be found in Levison et al. (2021).

To achieve these goals, the *Lucy* spacecraft carries a primary science payload consisting of a multispectral camera, infrared imaging spectrometer, high-resolution panchromatic imager, and a thermal infrared spectrometer. Additionally, two spacecraft subsystems also act as secondary science payloads: the spacecraft's communications system will be used to determine the mass of each Trojan target via Doppler tracking, and a wider-field panchromatic camera system will be used to perform autonomous terminal tracking of the Trojan targets during the close approach subphase of each flyby. These Terminal Tracking Cameras (TTCams) are part of the guidance, navigation, and control subsystem of the Lockheed Martin spacecraft's Flight System (Cox et al. 2024), and are designed to help provide updated knowledge of the target locations for the spacecraft's science instruments mounted on the two-axis articulated Instrument Pointing Platform (IPP). However, the TTCams will also provide extensive imaging coverage over a wide range of phase angles immediately before, during, and after each flyby (after the system's terminal tracking function is complete), thus providing unique constraints on the shape and volume of each target as well as additional coverage of each target for geologic characterization and mapping. In turn, estimates of both the mass and volume will lead to an estimate of the density of each target. Additional details about the *Lucy* mission's science goals, payload, IPP, and mission operations concept can be found in Levison et al. (2021) and Olkin et al. (2021).

This paper describes the requirements, design, testing, and expected performance characteristics of the *Lucy* TTCam imaging system, with a focus on the instrument characteristics and performance that will enable the additional science results described above. Additional details about the specific timing and algorithms that will be used by the TTCam system for terminal tracking of each target are provided in Good et al. (2022), and additional details about the pre-flight and in-flight calibration of the TTCam system are provided in Zhao et al. (2024).

2 *Lucy* Terminal Tracking Camera Requirements

The driving science-relevant requirements for TTCam (Table 1) are set by the camera's primary function as a navigation system designed to provide an autonomous onboard late pre-encounter update of the location of each target relative to the spacecraft. By definition and "to do no harm" to the system's ability to achieve its primary target tracking function for the mission, Requirements 1 through 4 were defined as being fully adequate for TTCam images to be able to meet their secondary science requirements related to shape modeling/volume determination (e.g., Mottola et al. 2024) and additional geologic characterization (e.g., Marchi et al. 2023). Requirements 5 and 6 enable higher-fidelity images for science analysis as well as finer temporal (phase angle) sampling in the few minutes around each closest approach. Neither of these science-focused requirements will impact the ability of the TTCam system to meet its primary navigation and tracking function. Additional requirements and specifications for the TTCam system that are primarily related to the system's tracking function are described in Good et al. (2022).

Table 1 Science-Related Requirements for the *Lucy* Mission Terminal Tracking Camera System

1	Provide sufficient sensitivity to allow an image with a Signal to Noise Ratio (SNR) of ≥ 10 for a target with a radiance factor (I/F) of 0.0020 at a solar distance of 5.7 AU and for an integration time of ≤ 400 msec.
2	Have a Field of View (FOV) sufficiently large to completely encompass each target throughout each flyby.
3	Have an Instantaneous Field of View (IFOV) sufficiently small to resolve a target with visible dimensions of 52×45 km at 51,400 km distance and at a solar phase angle of 125° to greater than 4 pixels wide and 10 total pixels of area.
4	Acquire images of a V magnitude 6 star with $\text{SNR} > 5$ for a 10 second exposure.
5	Flat field images at $\text{SNR} > 100$ shall be generated during pre-flight ground calibration.
6	The cadence of image acquisition during the closest approach phase of each flyby (once the terminal tracking function has completed) shall enable $\leq 10^\circ$ sampling of solar phase angles.

Requirements 1 through 4 drive the choice of detector and its Quantum Efficiency (QE), the detector size and pixel pitch, the $f/\#$ of the optics, and the aperture size. For example, the driving case for Requirement 2 (Field of View: FOV) is the flyby of the (617) Patroclus/Me-noetius Trojan binary pair in 2033. The approximately equal-sized asteroids each have an estimated projected size on-sky of $\sim 122 \times 113$ km. Thus, for a nominal close approach flyby distance of ~ 1000 km, the TTCam FOV required to encompass each of these objects would need to be at least $\sim 10.8^\circ \times 8.1^\circ$, including a 25% to 45% margin to accommodate errors on the estimated diameter and spacecraft pointing. Further, given the rectangular aspect ratio of typical digital imaging sensors, the orientation of the camera on the spacecraft was chosen such that the wider axis is along the direction of the largest expected pointing errors. As another example, to obtain images at least 4 pixels wide of a 52×45 km object at 51,400 km distance (simulating an asteroid being tracked on approach) would require the optics to have an Instantaneous Field of View (IFOV) of $\leq \sim 253 \times 219 \mu\text{rad/pixel}$, with 219 μrad being the driving case minimum pixel scale for Requirement 3. Finally, Requirements 1 and 4 also provide specific constraints on the QE, read noise, gain, full well, and transmissivity of the optics that would be required to meet the specified extended source or point source SNR levels.

Requirement 5 (flatfields for science) was designed to be met by increasing the number of flatfield images acquired for each camera during pre-flight calibration to increase the SNR of co-added flatfield images via simple photon counting (square root of the number of images combined) statistics. Requirement 6 (phase angle sampling) is designed to enable excellent shape modeling of each target, and will be met by increasing the cadence of imaging of each target during the few minutes around closest approach, starting after the primary target tracking function of the system has completed. The stressing case for this requirement is the 2027 flyby of (15094) Polymele, where an imaging cadence of ~ 13 seconds between subsequent images will be required to enable solar phase angle sampling in increments of $\sim 10^\circ$.

3 Target Tracking and Optical Navigation Support Objectives

As described in Good et al. (2022), the TTCam's primary role in the *Lucy* mission is to provide center-of-body measurements that allow the encounter solution to converge on the range to the target asteroid. *Lucy*'s science observations during the close approach phase

of each encounter are range-triggered and an accurate solution is required to achieve *Lucy* science objectives.

In addition, the *Lucy* Navigation team will use TTCam images taken within the minutes surrounding each encounter close-approach for trajectory reconstruction. This was added to the baseline optical navigation (OpNav) plan during development, in order to meet the Trojan closest approach radial distance accuracy requirement. Additionally, the OpNav team will characterize the in-flight optical distortion and boresight alignment of the TTCams relative to the L'LORRI boresight (see Sect. 7.2 and Zhao et al. 2024).

4 Design Considerations and Heritage

In addition to meeting the specific performance requirements identified in Table 1, other important objectives in the selection of a specific implementation of the TTCam imaging system were to minimize size, mass, and power requirements as well as cost, and to maximize system heritage acquired from previous deep space missions. Given those constraints, Lockheed Martin Flight System engineers and managers chose to procure an imaging system developed by Malin Space Science Systems, Inc. (MSSS; San Diego, CA) that is based on their ECAM line of science-grade polychromatic cameras (MSSS 2013; Ravine et al. 2016). The CMOS sensor, camera acquisition and storage/processing electronics, and camera flight software and logic chosen for TTCam have high heritage from the TAGCAMS imaging system flown successfully on the NASA OSIRIS-REx mission (Bos et al. 2018, 2020) and the Junocam imaging system flown successfully on the NASA Juno mission to Jupiter (Hansen et al. 2017). The optics design ultimately selected for the TTCam system is a unique prescription designed to specifically meet the *Lucy* mission requirements, but is based on many previous MSSS-developed deep space refractive optical designs.

5 Instrument Description

5.1 CMOS Sensor and Camera Head Electronics

Figure 1 shows the basic block diagram for the two fully block redundant TTCam camera heads and their associated Digital Video Recorder (DVR) electronics cards (each known as a “slice”). The heart of each TTCam is a 2752×2004 pixel monochrome CMOS imaging sensor from Aptina/ON Semiconductor (Model MT9P031). The sensor has $2.2 \mu\text{m}$ pixels and is operated at 10 MHz clock rate in Electronic Rolling Shutter mode, resulting in a ~ 680 msec full-frame readout time from the top to bottom row of each image (ON Semi 2017). On-chip electronics convert amplified photon-induced voltages to digital signals with a 12-bit dynamic range (Data Numbers or DN from 0–4095) and a selectable analog gain from $1 \times$ to $3 \times$ for this implementation. The QE of the detector ranges from $\sim 55\%$ to $\sim 35\%$ over the 425 to 675 nm bandpass of the system, with a peak of $\sim 62\%$ near 470 nm (ON Semi 2017).

Due to a limit on the image size that can be transferred into the spacecraft’s terminal tracking algorithm, only the pixels in the 2592×1944 active (light sensitive) image area are retrieved and used for imaging during terminal tracking mode observations (Fig. 2). For calibration mode images not taken during asteroid tracking, additional rows of masked pixels outside of the active area are downlinked to provide 2592×2000 pixel images that enable assessment of the bias plus dark current background signal levels over time and temperature.

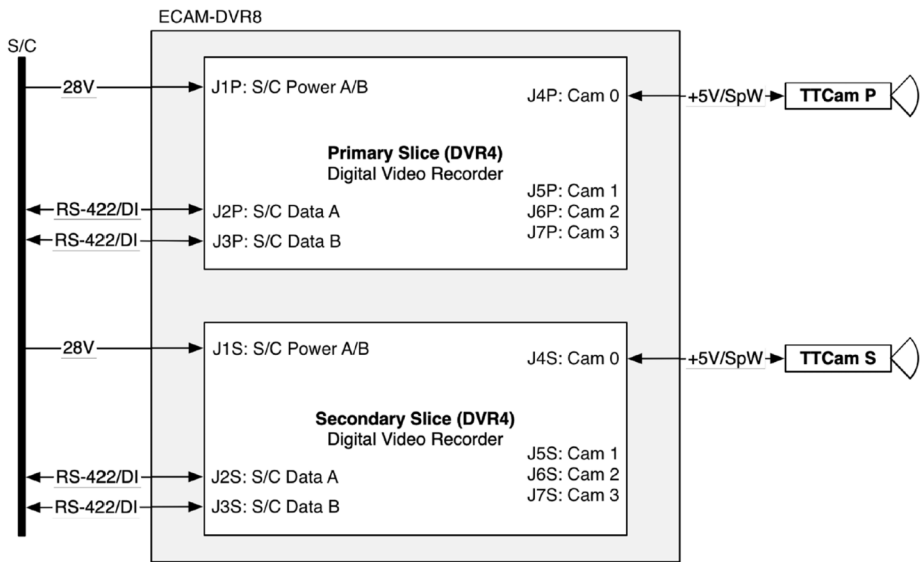


Fig. 1 TTCam electronics block diagram. Additional external harnessing for thermal control is not shown

These calibration mode images provide a way to validate a model (Zhao et al. 2024) for the removal of these effects in the calibration of the 2592×1944 terminal tracking mode images lacking masked pixels.

Based on the *OSIRIS-REx* TAGCAMS experience using this same sensor (see Bos et al. 2020 Fig. 6 and its associated text), only the masked pixels in rows 1966 to 1989 and columns 16 to 2607 in Fig. 2 are used for the assessment of background signal level in calibration mode images that contain masked pixels. For asteroid tracking and encounter images downlinked without masked pixels, a modeled background is used to remove that background signal from the raw data (see Sect. 6.1 below and Zhao et al. 2024).

The TTCam sensors are controlled by dedicated electronics in each camera head assembly. The camera head electronics are built around a rad-hard FPGA that performs all logic functions, including CMOS sensor power control, clock generation, and command and SpaceWire interfaces. In addition, the FPGA can perform a limited amount of pixel processing, including 12-bit to 8-bit companding (see Sect. 5.3), prior to transfer of imaging data to the DVR.

5.2 Digital Video Recorder (DVR)

The TTCam DVR receives +28 V of nominal bus voltage and receives commands from the *Lucy* spacecraft, provides switched +5 V of power to the CMOS sensors and camera head electronics, and captures image data from the camera heads over a SpaceWire interface. Camera-specific flight software and logic developed by MSSS is loaded into each slice of the DVR and runs on a Microblaze soft processor within a Xilinx FPGA. The DVR controls the storage of images in flash memory (up to ~ 1600 uncompressed 8-bit full-sensor images can be stored per camera) and the transmission of image data as well as health and status telemetry back to the spacecraft computer via an RS-422 asynchronous serial interface. The DVR also runs internal fault management (including single-event-upset mitigation) and can

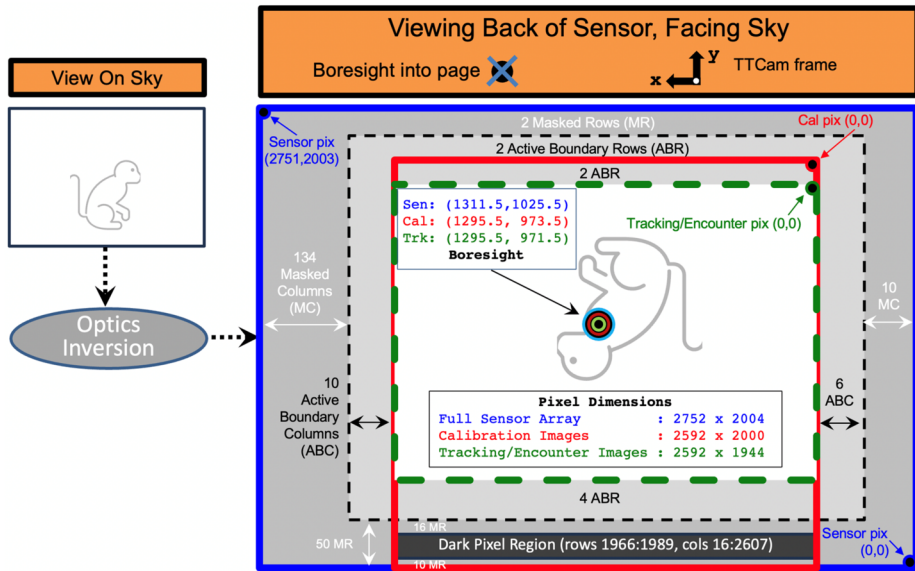
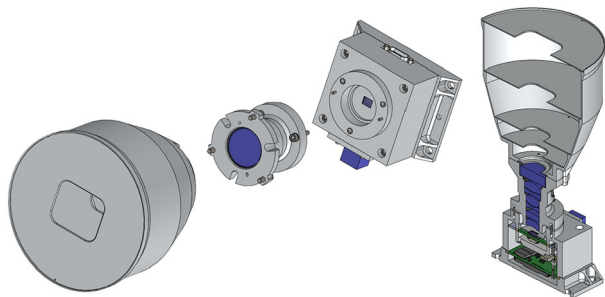


Fig. 2 Cartoon diagram of the full TTCam1 CMOS detector array as it is oriented in the TTCam coordinate frame, showing the full sensor coordinate system (blue outline), and the pixel areas and TTCam coordinate system for downlinked images in Calibration Mode (red outline) and in Tracking/Encounter Mode (green outline). Pixel area dimensions are not to scale. The sensor's active image area is in white, the active (un-masked) boundary pixel area is in light gray, the masked pixel area is in dark gray, and the masked pixel area used for bias and dark current assessment is in black. An image of a simian is shown as it appears on the sky and as it is projected onto the sensor array by the instrument optics. All indexing is 0-based center-of-pixel. The vertical (y) axis of the downlinked images runs anti-parallel to the sensor array coordinates. The sensor geometry is the same for TTCam2, but the camera and images are rotated 180° about the optical axis relative to TTCam1

Fig. 3 CAD model of the three main components of the TTCam camera head and cutaway view of the integrated system



perform optional onboard lossless (Huffman first-difference) or lossy (JPEG) compression. The DVR contains two independent slices, one per camera head, in a single aluminum housing. Each slice contains redundant data connectors to enable it to interface with either the primary or backup *Lucy* flight computer.

5.3 Optomechanical Design

Figure 3 shows a CAD model representation of the three main components of each TTCam camera head: electronics box, optics assembly, and sunshade. The electronics box (which

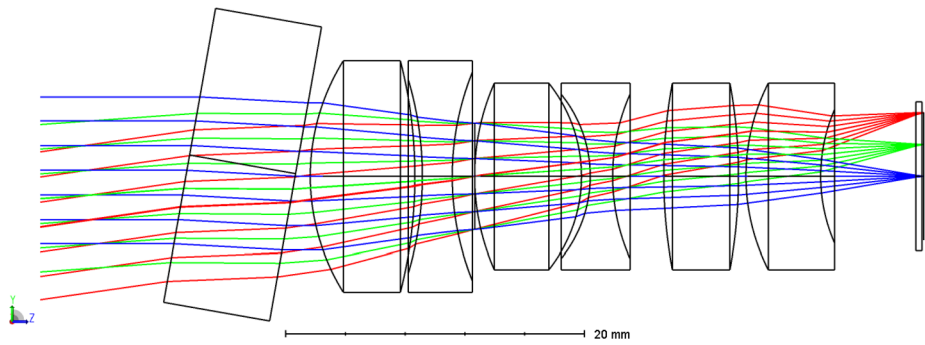


Fig. 4 TTCam optics ray trace. The front window is intentionally tilted by $\sim 5^\circ$ to help mitigate stray light

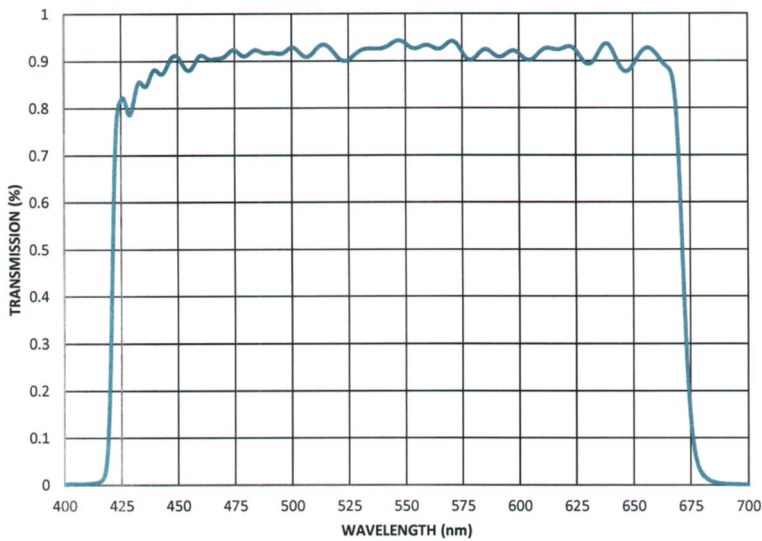
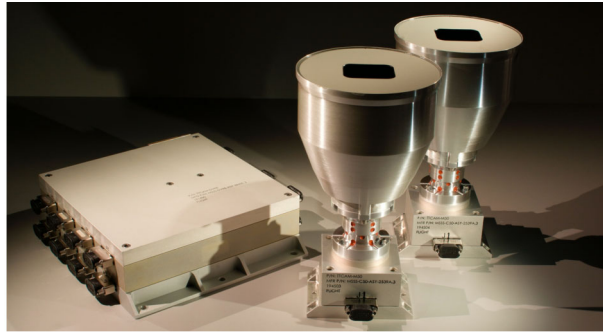


Fig. 5 Overall transmission of the TTCam optics + bandpass filter as a function of wavelength

houses the CMOS sensor and its FPGA electronics) uses the same mechanical design as that used on the OSIRIS-REx TAGCAMS (Bos et al. 2018).

MSSS subcontracted to Collins Aerospace (Carlsbad, CA) for the TTCam lens design, fabrication, and component-level testing. The optics (Fig. 4) consist of a seven-element refractive design, including an intentionally-tilted front window to help mitigate stray light. In addition, a 425–675 nm bandpass filter (Fig. 5) is part of the tilted front window, to enable broad-band imaging in the wavelength region where the sensor QE is highest. The TTCam optics are designed to be athermal over the expected operating temperature range of the cameras (-40°C to $+55^\circ\text{C}$). The optics alone were required to meet a 30% Modulation Transfer Function (MTF) requirement at the Nyquist frequency (227 line pairs/mm), and the overall system (optics + filter + CMOS sensor) was required to have an MTF greater than 10% at Nyquist. Despite the relatively wide field of view, distortion in the lens design is expected to be very small, only $\sim 0.12\%$ in the corners of the field. Stray light in the system is also expected to be extremely small, with the strongest ghost images predicted to have an

Fig. 6 Photo of the *Lucy* TTCam flight Digital Video Recorder (left) and the two flight camera head electronic boxes and sunshades (from left to right: serial numbers 194503 – the Primary camera – and 194504 – the Secondary camera). For scale, the DVR is $19 \times 16 \times 7$ cm in size and each camera head electronics box is 8×8 cm square.



intensity of 0.5% or less of the primary image. These very small distortion and stray light levels have been validated in flight (Zhao et al. 2024).

5.4 Onboard Image Processing

Onboard processing of raw TTCam images is performed both within the DVR flight logic prior to transferring the images to the *Lucy* spacecraft, and then within the spacecraft flight software itself, after image transfer but prior to eventual downlink. First, the raw 12-bit DN values in each pixel are compressed to 8-bits, nominally using an onboard square-root lookup table designed to avoid Poisson (shot) noise being encoded or downlinked in the telemetry (a process known as “companding”; e.g., Malin et al. 2013; Bell et al. 2017). For some cruise image tests of different companding schemes, the 12-bit to 8-bit compression is achieved either using a divide-by-16 linear scaling, or by clipping the 12-bit images down to just their least-significant 4 bits. Then, the 8-bit companded but otherwise uncompressed images are transferred to the spacecraft computer, where they are further compressed using the lossless PPMd algorithm (Prediction by Partial Matching, variant d; e.g., Jumar et al. 2018) to further decrease the average number of bits per pixel to be downlinked.

5.5 Integration and Accommodation

Figure 6 shows the TTCam flight DVR and camera heads (Primary = DVR1 = serial number 194503; Secondary = DVR2 = serial number 194504). Additionally, two ~ 76 cm harnesses fabricated by Glenair (Glendale, CA) connect each slice of the DVR to its corresponding camera head. The camera head electronics box, optics module, and sunshade were integrated at MSSS in the winter and spring of 2020, and a series of ambient and thermal vacuum condition Verification and Validation (V&V) and calibration tests were performed at MSSS in June and July, 2020 (see Sect. 6 and Zhao et al. 2024). The flight DVR and flight camera heads were delivered to the Lockheed Martin *Lucy* mission Assembly, Test, and Launch Operations (ATLO) team in July, 2020, and were installed on the spacecraft’s Instrument Pointing Platform shortly thereafter (Fig. 7). For harness and connector accommodation, TTCam1 and TTCam2 are rotated by 180° about the optical axis relative to each other, and thus the entire sky to sensor to downlinked image coordinate frame relationship shown in Fig. 2 is repeated for TTCam2, but rotated 180° relative to TTCam1. As described in more detail in Olkin et al. (2021) and Good et al. (2022), both the Primary and Secondary TTCams are co-boresighted with the rest of the *Lucy* instruments, and all instrument FOVs are completely contained within the TTCam FOVs.



Fig. 7 Photo of the Lucy TTCam1 (T1) and TTCam2 (T2) flight cameras (with red “Remove Before Flight” covers) installed on the spacecraft’s Instrument Pointing Platform. The large cylinder to the upper left of T1 is the L’ORRI telescope (L), and the smaller black cylinder below T2 is the telescope for the L’TES infrared spectrometer (TES) [see Olkin et al. (2021) and Good et al. (2022) for additional instrument and spacecraft details]. Photo taken in Aug. 2021 at Lockheed’s pre-launch integration facility at Cape Canaveral, Florida, and used with permission of Lockheed

6 Expected Instrument Performance

6.1 Preflight Predictions

During the design phase of the TTCam development process, a model was generated to predict the SNR that could be achieved for Trojan asteroid targets imaged by the TTCam system. Known/verifiable parameters in the model included the QE, read noise, gain, and dark current rate of the sensor, the transmission of the optics, and the flyby speed at each encounter (to factor in potential image smear). Assumed or variable characteristics of the model included the heliocentric distance of the observations, and the nature of the surface phase function of the target asteroids. Table 2 shows an example of the resulting SNR predictions for TTCam observations of each of the *Lucy* flyby targets for assumed Lambertian (“Albedo” columns) and Lommel-Seeliger (“LS” columns) surface phase functions. These predictions, since validated from Earth and Moon observations in flight (see Sect. 7.2 and Zhao et al. 2024), provide confidence that the actual flight cameras would be able to meet the SNR requirements specified for the system (Table 1).

6.2 Preflight Characterization Measurements

After subsystem integration and initial functional testing, the two flight and one flight spare (serial number 194501) TTCams went through an ambient and thermal vacuum V&V and calibration testing program at MSSS that included assessments of CMOS sensor and electronics gain, read noise, linearity/full well, and dark current rate, as well as system radiometry, bandpass performance, flatfield behavior, and assessments of MTF and FOV/distortion. Detailed stray light measurements and modeling were also conducted during ATLO (see

Table 2 Predicted SNR from *Lucy* TTCam observations of each of the Trojan flyby targets

Body – Trojan Swarm	Average Diameter (km)	Solar Phase (°)	Encounter Velocity (km/s)	Stability (°/s)	Closest Approach (km)	Sun Range (AU)	Dia./FOV @C/A	IFOV (m/pix)	Exp. Time (ms)	Albedo Model	Albedo SNR	LS Model	LS SNR
Eurybates – L ₄	46.4	81	5.8	0.09	1000	5.7	0.32	74.1	20.0	0.050	47.4	0.077	59.3
Polymele – L ₄	15.1	81	6.0	0.27	400	5.7	0.26	29.6	20.0	0.090	64.2	0.077	59.3
Leucus – L ₄	65	104	5.9	0.09	1000	5.6	0.45	74.1	20.0	0.080	61.5	0.087	64.2
Orus – L ₄	31	126	7.1	0.09	1000	5.3	0.22	74.1	20.0	0.080	65.1	0.086	67.5
Patroclus/ Menoetius – L ₅	132/ 122	56	8.8	0.09	1244/ 1074	5.4	0.79/ 0.74	92.2/ 79.6	20.0	0.047	50.5/ 48.5	0.058	54.1/ 56.3

Sect. 6.3) to take into account the potential scattered light effects of other payload elements and subsystems on the IPP and spacecraft. Details and results from many of these pre-flight tests and analyses are described in Zhao et al. (2024), and Table 3 summarizes the resulting derived or measured properties and characteristics of the TTCam system.

6.3 Assembly, Test, and Launch Operations (ATLO) Testing

Testing in ATLO was primarily driven by the terminal tracking needs of the mission. The minimum focal distance of the TTCams (~200 m) precluded meaningful imaging in the ATLO test environment, so pre-made images were loaded onto the DVR to be sent to the spacecraft during testing. See Good et al. (2022) for a discussion of the image simulation and testing.

Additional scattered light testing was done during ATLO as part of a larger, mission level scattered light test. Earlier simulations had indicated that sunlight might be reflected from the L'LORRI baffles in certain orientations of the spacecraft on approach or departure from a target. Testing was done with a setup designed to simulate the various potential Trojan encounter geometries (Fig. 8). Actual scattered light levels were much lower than predicted by the earlier modeling, and thus scattered light is predicted to have no impact to either science or terminal tracking functionality. This prediction has been validated from dedicated cruise scattered light characterization observations (see Sect. 7.2 and Zhao et al. 2024).

7 Mission Operations and Data Products

7.1 Operational Considerations

Because the flyby velocities are so high (~6–9 km/sec) and the encounters occur so far from Earth (42 to 47 light-minutes), the primary function of the TTCam imaging system is to provide an important late (shortly before each flyby) update of the location of each target asteroid relative to the *Lucy* spacecraft (Cox et al. 2024). TTCam's navigation and tracking function will thus enable more accurate pointing of the much higher-resolution and smaller-FOV instruments on the *Lucy* science payload. Since the system will have completed that job at least several minutes before each close approach but will continue collecting images throughout the entire encounter, TTCam images will also be available to help fulfill some of the science objectives of the *Lucy* mission as well.

Operationally, however, using TTCam during the close approach phase of each flyby will involve a change in data collection cadence. Specifically, TTCam images used for the Flight

Table 3 *Lucy* Mission Terminal Tracking Camera (TTCam) Specifications

<i>Optics</i>	<i>Description</i>
Focal length	29.7 mm (all-refractive; fixed focus)
Focal ratio	$f/2.95$
Depth of Field	≈ 200 m to ∞ (hyperfocal: 133.7 m; near-focus: 66.8 m)
entrance pupil aperture	9.9 mm
aperture area	77 mm ²
exit pupil diameter	7.1 mm
t/#	< 3.36
pixel solid angle	5.5×10^{-9} sr
throughput ($A_0 \bullet \Omega$)	4.22×10^{-7} mm ² sr
IFOV	74.1 μ rad/pixel (74.1 m/pixel @ 1000 km)
FOV	11.0° \times 8.2° (13.7° diagonal) (193 \times 143 km @ 1000 km)
Filters	1
Filter bandpass	Panchromatic: 425-675 nm
Effective Wavelength	Avg. Red Trojan: 537.8 nm (FWHM: 246.7 nm)
(Filter \times QE \times Sun \times Trojan)	Avg. Less-Red Trojan: 534.1 nm (FWHM: 245.2 nm)
Optics Transmission	> 80%
Optics Distortion	0.12% average in corners of field of view
MTF	0.19 (optics+filter+sensor) at Nyquist = 227 l.p./mm
<i>Detector & Electronics</i>	<i>Description</i>
Sensor	CMOS: ON Semi Model MT9P031; Electronic Rolling Shutter mode
Clock Rate	10 MHz in 8-bit mode
Exposure Durations	~ 0.0 to 30.7675 sec; commanded in units of 0.1 msec
Electronic Rolling Shutter	Min. exp.: 121 or 60.4 μ sec (8-bit or 12-bit); Frame time ~ 680 msec
Array size	2592 \times 1944 active pixels (2752 \times 2004 total)
Preferred Dark Pixels (cf. Fig. 2)	rows 1966-1989, cols 16-2607 (region 4 of Fig. 6 in Bos <i>et al.</i> , 2020)
Pixel size	2.2 μ m (square pixels)
Gain, Read Noise, Full Well	1.8 e ⁻ /DN; 7 e ⁻ ; 5400 e ⁻
Quantum Efficiency	> 50% at 550 nm
Digitization	12 bits/pixel; single gain, no offset states
DVR to Camera data interface	SpaceWire, 100 Mbit/sec
DVR-S/C Cmd/Housekeeping interface	RS-422, 57.6 Kbit/sec Asynchronous Serial
DVR-S/C video telemetry interface	RS-422, 8.33 Mbit/sec Synchronous Serial
Memory	8 GB non-volatile RAM (≈ 1600 8-bit images) per camera
Camera Head Power	1.5 W standby and 2.0 W imaging, per camera head
DVR Power	6.0 W standby and 8.0 W imaging, per camera board
<i>Image Compression Options</i>	<i>Description</i>
Uncompressed	12-bit data (0-4095 DN); No compression
Lossless	In DVR: First-difference, Huffman; In spacecraft: PPMd
Lossy	In DVR: JPEG, commandable compression quality (1–100)
Companding	In DVR: 12-bit to 8-bit square-root encoding (lookup table)
<i>Physical</i>	<i>Description</i>
Data Volume: full raw image	2752 \times 2004 \times 12 bits = 8.27 MBytes/image
Data Volume: 8-bit companded	2752 \times 2004 \times 8 bits = 5.52 MBytes/image
Data Vol: 8-bit then lossless comp.	2.76 MBytes/image, assuming 2:1 lossless compression
Dimensions: CMOS Sensor	5.7 \times 4.3 mm (7.1 mm diagonal)
Dimensions: Camera Head	8 \times 8 \times 22 cm (each camera)
Dimensions: DVR	19 \times 16 \times 7 cm
Mass: Camera Head	0.53 kg, CBE (each camera)
Mass: DVR	1.90 kg, CBE

System's navigation and tracking function will be acquired at a cadence of approximately 15 seconds per image, starting several hours before closest approach. Those tracking and encounter images will be rapidly transferred from the camera head to the DVR and into

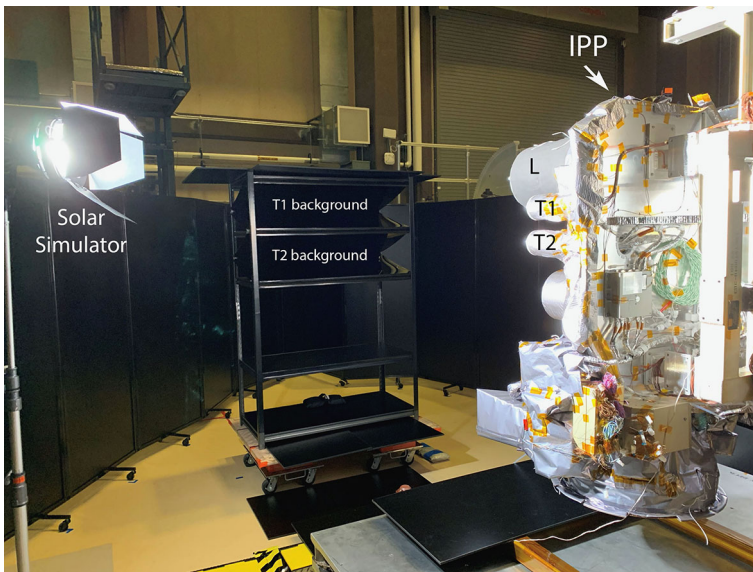


Fig. 8 Photograph of the setup used for TTCam stray light image testing during ATLO on May 6, 2021 at the Lockheed Spacecraft facility in Littleton, CO, and used with permission of Lockheed. The solar simulator lamp was oriented at different positions to simulate the viewing geometries of the Instrument Pointing Platform (IPP) during the various encounters. The fields of view of the Primary TTCam (T1) and Secondary TTCam (T2) were filled by dark background targets. Models had predicted that sunlight scattering off the L’LORRI telescope baffle (L) might produce contaminating background signature in the TTCams that could interfere with their tracking and navigation function. The actual tests showed extremely low scattered light levels in all simulated geometries, however

the spacecraft computer in 8-bit companded mode without the masked dark pixels. These smaller images are required because of a limit on the image size that can be transferred into the spacecraft’s terminal tracking algorithm. Once the tracking function is complete, however, (typically around 2 minutes before close approach), the cadence of TTCam imaging can be increased to provide the required phase angle sampling of each target (Requirement 6 in Table 1). These “science phase” TTCam images will also not include the masked pixel area of the CMOS array, because the images will still be getting acquired as part of the earlier navigation and tracking sequence.

Separately, as part of periodically executed in-flight calibration campaigns begun shortly after launch and expected to continue before and after the Trojan flybys (see Sect. 7.2), we are acquiring nearly full-sensor calibration images of star fields and the Earth and Moon that do include the masked pixel area. These calibration images are being used to validate the pre-flight radiometric calibration predictions for the TTCams, to monitor their performance over time, and to adjust the dark current models and/or bad pixel maps for the cameras, if needed (Zhao et al. 2024).

Many more details about the operational use of TTCam and the other *Lucy* payload elements can be found in Olkin et al. (2021) and Good et al. (2022).

7.2 In-Flight Calibration Observations and Plans

Since launch, a series of in-flight observational tests have been initiated to test and validate the performance of the TTCams to the fidelity necessary to perform the required asteroid

tracking, navigation reconstruction, and science tasks. The results from these calibration activities are being used to refine the calibration pipeline before reaching the first Trojan asteroid, as well as to provide valuable performance metrics for planning each encounter (Zhao et al. 2024).

The first TTCam functional checkout was performed just 20 days after launch, and ensured that the instruments were in good health. Star field exposures varying from 0.0 to 30.0 seconds provided a first opportunity to measure the detector bias, read noise, and dark current when temperatures were near their highest (near 1 AU). Additional star field and stellar cluster imaging was conducted 120 days and 7 months after launch, to validate the geometric calibration of the cameras and to test various image companding modes that could be used throughout the remainder of the mission's long cruise phase. Detector and optics performance will continue to be measured periodically during flight, and especially important will be observations planned during a series of 4 AU deep space calibration activities, when the thermal conditions are expected to more closely match the Trojan encounter temperature profiles.

A special set of TTCam observations was acquired during the first Earth Gravity Assist (EGA1) flyby one year after launch, to validate the radiometric calibration of the TTCams primarily based on imaging of the Moon. TTCam observations during EGA1 provided a successful demonstration of IPP pointing and TTCam extended source image quality (Fig. 9), as well as the required validation of the instrument's calibration pipeline and radiometric calibration coefficients, which yielded derived radiance factor (I/F, an approximation of surface reflectivity; Hapke 1993) values of high and low albedo lunar terrains that are within $\sim 15\%$ or less of their expected modeled I/F values (Zhao et al. 2024). More details about the *Lucy* EGA1 observations and results can be found in Spencer et al. (2023).

Among the more critical engineering in-flight activities has been a series of IPP calibration alignment sequences conducted during the launch + 120 days and EGA1 flyby. The purpose of these activities has been to determine the relative alignments between the TTCams and the L'LORRI and L'TES fields of view, as well as to fine-tune the alignment knowledge between the IPP and the spacecraft's star trackers. To perform this activity using star fields, a preliminary optical distortion calibration was required to effectively solve for the instrument boresights in each image. The observations conducted 120 days after launch, for example, consisted of slewing the IPP gimbal angles through 8 target fields (6 on the inner gimbal, and 2 on the outer gimbal.) These target fields were selected to maximize the number of stars captured in the TTCam and L'LORRI FOVs, within operational constraints. The images were processed through the KinetX camera calibration suite (Pelgrift et al. 2018) to estimate the distortion model parameters and focal length, such that the residuals are zero-mean with a standard deviation in both image dimensions on the order of the expected uncertainty in the center-finding algorithm, and showing no systematic structure related to the stars' positions within the FOV. In-flight assessment of geometric distortion has met pre-flight design and testing expectations, and initial results from early cruise are provided in Zhao et al. (2024).

Such observations also establish the TTCam coordinate system to spacecraft coordinate system pointing matrix and also provide the initial post-launch calibration of the optical distortion of the cameras over the usable FOV to better than 1 pixel at the edge of the FOV ($< 0.05\%$ of the focal length). The post-launch value of the camera focal length is also estimated as part of the solution for the distortion model parameters. By performing these observations near 1 AU and then again at 4 AU, we will also quantitatively characterize the sensitivity of the alignment and distortion calibrations to camera operating temperature and begin to establish if this calibration changes as the cameras age.

Fig. 9 Examples of TTCam images of the Earth and Moon acquired as part of the EGA1 imaging tests on Oct. 16, 2022. Insets show enlarged views



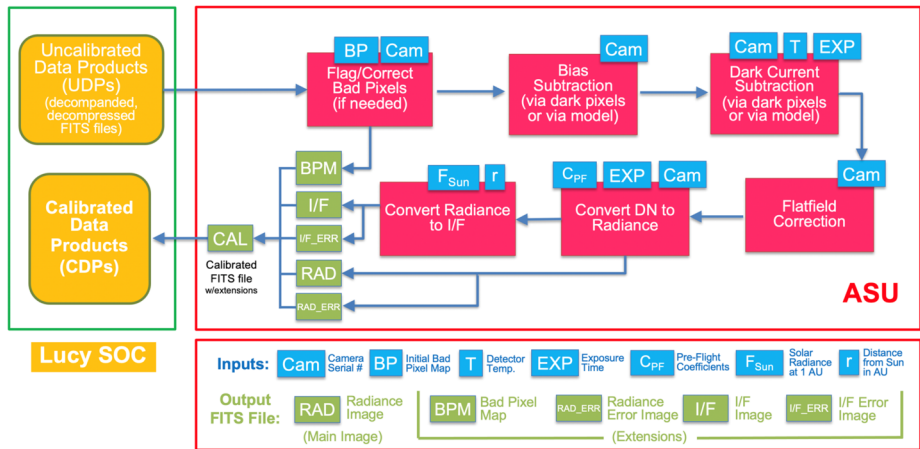


Fig. 10 Flow chart describing the TTCam ground data calibration pipeline. Inputs (in blue) include the camera ID, initial bad pixel map, CMOS detector temperature, exposure time, pre-flight radiometric conversion coefficients, the solar radiance at 1 AU convolved over the TTCam bandpass, and the heliocentric distance of the target object. See Zhao et al. (2024) for detailed descriptions of the pipeline outputs (in green)

Stray and scattered light characterization activities are also being performed during cruise, the first of which occurred almost 18 months after launch at 1.7 AU, and a second set in colder thermal conditions will be acquired once the spacecraft reaches 4 AU. These tests, as well as pre-flight scattered light tests (Sect. 6.3), provide images that provide a qualitative assessment of the expected magnitude of stray and scattered light in TTCam images at the most challenging expected encounter geometries for the *Lucy* asteroid target encounters. The initial 1.7 AU tests confirmed the expectation based on the optics design (Sect. 5.4) that scattered light will not be a significant contributor to the signal in TTCam tracking or encounter images acquired at the expected few to tens of millisecond exposure times (Zhao et al. 2024).

7.3 Ground Data Processing and Calibration

The TTCam calibration pipeline, which is part of the *Lucy* mission's Science Operations Center (SOC), takes in uncalibrated data products (UDPs) in Flexible Image Transport System (FITS) format and turns them into calibrated data products (CDPs), also as FITS files, and including extensions. Figure 10 shows a basic flowchart of the calibration pipeline. The pipeline takes in, as input, a list of UDPs, and uses UDP header information to find the relevant calibration files and parameters needed for each flight model. The pipeline outputs the CDP as a single FITS file, with the main FITS image containing the derived radiance of the scene, plus four FITS extensions that contain: (1) a bad pixel map; (2) a radiance error image; (3) an I/F image; and (4) an I/F error image. Details on the inputs, algorithms, and outputs of this calibration pipeline are provided by Zhao et al. (2024).

7.4 Expected Science Analyses and Data Products

Although primarily a spacecraft subsystem, because of its relatively wide angle FOV, large pixel count, and high-cadence capabilities, TTCam offers an invaluable complement to the mission's narrow-angle imagers for achieving *Lucy*'s science goals. Especially during the

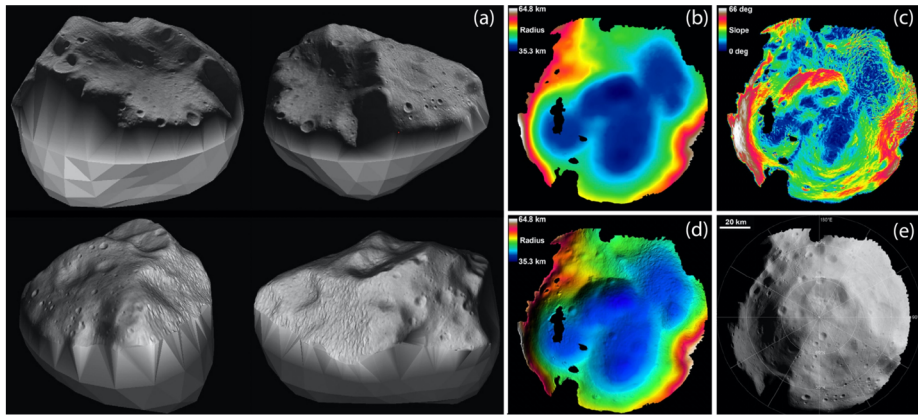


Fig. 11 (a) Textured shape model of asteroid (21) Lutetia obtained partly from Rosetta OSIRIS images comparable to what we expect from the Lucy TTCam images (Preusker et al. 2012). Also shown are other example derived products from OSIRIS images, including (b) a color-coded Digital Terrain Model; (c) a slope map; (d) a hill-shaded relief map; and (e) an orthoimage mosaic. All panels in Lambert Azimuthal Equal-area projection and based on Preusker et al. (2012)

few minutes immediately before and after the respective closest encounters with each target, TTCam will be able to image the entire sunlit part of each body within a single frame and capture the rapidly changing viewing geometry during the flyby. As described below, these observations will help address a number of specific *Lucy* mission science goals. In addition to the systematically processed calibrated images, TTCam data will also be released in the form of higher-level products such as controlled and uncontrolled mosaics, ortho-rectified maps, local Digital Terrain Models (DTMs), thematic maps, rendered views, and fly-over movies.

7.4.1 Trojan Asteroid Shape Modeling and Volume Estimation

TTCam flyby images of each Trojan target body from different perspectives, together with the data from the other *Lucy* imagers, will enable the generation of shape models and DTMs by means of methods like stereophotogrammetry and photoclinometry (e.g., Capanna et al. 2014; Mottola et al. 2024) as well as limb and terminator tracking. For flybys during which the spin state of the object (spin rate and axis orientation) prevents the observation of the whole target, the shape model will be complemented with a ground-based model obtained through lightcurve and stellar occultation observations, as done for example by Preusker et al. (2012) for the *Rosetta* mission (21) Lutetia flyby (Sierks et al. 2011).

The shape models derived from TTCam images and other data will provide the basis for the determination of the size, volume, and refinement of the rotation properties of the targets (e.g., Fig. 11). The volume determination, in conjunction with the mass estimation from the radio-science experiment, will enable the determination of the object's bulk density. The presence of a misalignment between the figure principal axis and the spin axis would give hints about the internal mass distribution. Furthermore, by providing information about the local illumination and viewing conditions on the surface, the shape model will enable photometric studies to be performed, to reveal the physical properties of the regolith.

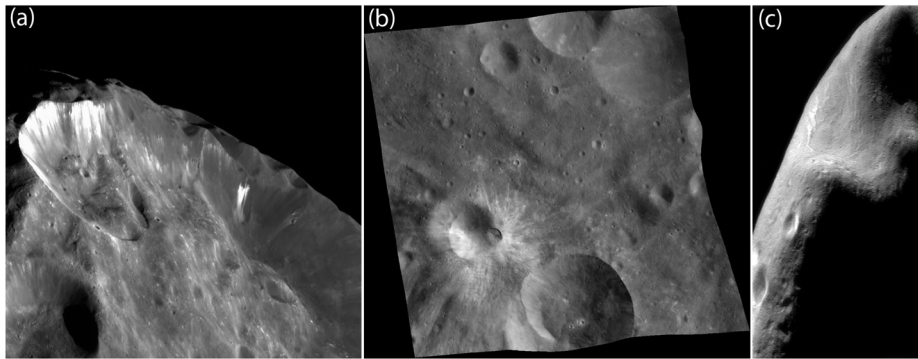


Fig. 12 Example images of small bodies all at the typical expected image scale (~ 70 m/pix) of TTCam Trojan close approach images. (a) Impact cratering surface gradation processes on Saturn's moon Phoebe, from the Cassini mission (JPL Photojournal image PIA06075); (b); Impact cratering, subsurface exhumation, and surface degradation processes on part of main belt asteroid (4) Vesta, from the Dawn mission (Dawn image F2_372565839); and (c) Impact and potential tectonic processes on the near-Earth asteroid (433) Eros, from the NEAR-Shoemaker mission (NEAR image M0126540610F4)

7.4.2 Trojan Asteroid Geology and Topography

As described by Olkin et al. (2021) and Marchi et al. (2023), an important additional scientific use of TTCam images of the *Lucy* target asteroids will be to help characterize their geology and geologic history. Given the field of view and pixel scale of the TTCams, and the planned flyby distances, none of the Trojan targets are expected to over-fill the TTCam field of view. Thus, the TTCam image data set for each flyby will provide “whole disk” views of the entirety of the sunlit surface of each target body, at pixel scales around 30 to 90 m/pixel, depending on the specific flyby distances.

Even though TTCam images will have much lower resolution than those from the other *Lucy* science payload imagers, they will provide superior coverage of each Trojan target, and will thus directly address a number of specific *Lucy* science goals (Levison et al. 2021). For example, as shown in Fig. 12, imaging at typical TTCam pixel scales can allow a global assessment of the morphology, size distribution, and areal distribution of impact craters on small bodies. In addition, TTCam images could provide evidence for other albedo features and/or geologic structures or units that could be potentially indicative of erosional, tectonic, or perhaps even cryovolcanic processes on Trojan asteroids. Finally, the multiple emission angle views of each target provided by TTCam imaging during the flyby will enable the creation of stereoscopic images and DTMs for a significant fraction of the sunlit surface.

8 Summary

This paper summarizes the requirements, design, expected in-flight performance, in-flight calibration plans, and expected science potential of the NASA *Lucy* Trojan asteroid Discovery mission's Terminal Tracking Camera (TTCam) imaging system. The details of the optics, electronics, and the calibration and performance information provided here is primarily focused on the eventual scientific use of TTCam images to contribute to the mission's overall science goals (Levison et al. 2021). Additional details about the use of the TTCam system for their primary *Lucy* mission function – as a navigation system designed to provide

an autonomous onboard late pre-encounter update of the location of each asteroid target relative to the spacecraft – can be found in Olkin et al. (2021) and Good et al. (2022), and the technical details on the pre-flight and in-flight calibration of the cameras can be found in Zhao et al. (2024).

Acknowledgements We are extremely grateful to the members of the *Lucy* mission team, MSSS staff, NASA support staff, and their many subcontractors and vendors who kept the design, development, fabrication, and testing of the TTCam system on track despite the numerous hardships and risks associated with the 2020–2021 global CoVID-19 pandemic. We thank Danielle Smilovsky and Oketa Basha (ASU) for support on the development and testing of the TTCam instrument calibration pipeline, and Jeanne Ladewig at Lockheed Martin for her many years of support of TTCam design, development, and integration.

Funding This work was funded by grants and contracts from the NASA *Lucy* Discovery mission.

Declarations

Competing Interests The authors have no competing or financial interests to declare that are relevant to the content of this article.

Open Access This article is licensed under a Creative Commons Attribution 4.0 International License, which permits use, sharing, adaptation, distribution and reproduction in any medium or format, as long as you give appropriate credit to the original author(s) and the source, provide a link to the Creative Commons licence, and indicate if changes were made. The images or other third party material in this article are included in the article's Creative Commons licence, unless indicated otherwise in a credit line to the material. If material is not included in the article's Creative Commons licence and your intended use is not permitted by statutory regulation or exceeds the permitted use, you will need to obtain permission directly from the copyright holder. To view a copy of this licence, visit <http://creativecommons.org/licenses/by/4.0/>.

References

- Bell JF III, Godber A, McNair S, Caplinger MA, Maki JN, Lemmon MT, Van Beek J, Malin MC, Wellington D, Kinch KM, Madsen MB, Hardgrove C, Ravine MA, Jensen E, Harker D, Anderson RB, Herkenhoff KE, Morris RV, Cisneros E, Deen RG (2017) The Mars Science Laboratory Curiosity rover Mastcam instruments: Preflight and in-flight calibration, validation, and data archiving 4:396–452. <https://doi.org/10.1002/2016EA000219>
- Bos BJ, Ravine MA, Caplinger M, Schaffner JA, Ladewig JV, Olds RD, Norman CD, Huish D, Hughes M, Anderson SK, Lorenz DA, May A, Jackman CD, Nelson D, Moreau M, Kubitschek D, Getzandanner K, Gordon KE, Eberhardt A, Lauretta DS (2018) Touch And Go Camera System (TAGCAMS) for the OSIRIS-REx Asteroid Sample Return mission. *Space Sci Rev* 214:37. <https://doi.org/10.1007/s11214-017-0465-2>
- Bos BJ, Nelson DS, Pelgrift JY, Liounis AJ, Doelling D, Norman CD, Olds RD, May CW, Witherspoon R, Church E, Huish D, Adam CD, Sahr E, Kidd J, Drozd K, Owen WM, Moreau MC, Seals LT, Butt J, LeDuc D, Alkie K, Chevres-Fernandez LR, Gordon KE, Khlopenkov K, Haney C, Bhatt R, Hikes J, Wolfram A, Caplinger M, Ravine MA, Getzandanner K, Bartels A, Lauretta DS (2020) In-flight calibration and performance of the OSIRIS-REx Touch And Go Camera System (TAGCAMS). *Space Sci Rev* 216:71. <https://doi.org/10.1007/s11214-020-00682-x>
- Capanna C, Jorda L, Gesquière G, Gaskell RW, Groussin O, Gutiérrez P, Hviid SF, Lamy PL, Preusker F, Rodionov S, Scholten F, Vibert D (2014) Multi-resolution stereophotoclinometry by deformation, a new 3D shape reconstruction method applied to ROSETTA/OSIRIS images. In: AGU fall meeting abstracts. P41C-3941
- Cox M et al (2024) The Lucy spacecraft. *Space Sci Rev* 220
- Good PG, Faiks P, Pisano WJ (2022) Terminal Tracking for the Lucy Trojan Asteroid Mission. In: 44th Annual AAS Guidance, Navigation and Control Conference. AAS 22-131. <https://ntrs.nasa.gov/citations/20220001851>
- Hansen CJ, Caplinger MA, Ingersoll A, Ravine MA, Jensen E, Bolton S, Orton G (2017) Junocam: Juno's outreach camera. *Space Sci Rev* 213:475–506. <https://doi.org/10.1007/s11214-014-0079-x>
- Hapke B (1993) Theory of reflectance and emittance spectroscopy. Cambridge University Press, New York

- Jumar R, Maaß H, Hagenmeyer V (2018) Comparison of lossless compression schemes for high rate electrical grid time series for smart grid monitoring and analysis. *Comput Electr Eng* 71:465–476. <https://doi.org/10.1016/j.compeleceng.2018.07.008>
- Levison HF, Olkin CB, Noll KS, Marchi S, Bell JF III, Bierhaus E, Binzel R, Bottke W, Britt D, Brown M, Buie M, Christensen P, Emery J, Grundy W, Hamilton VE, Howett C, Mottola S, Pätzold M, Reuter D, Spencer J, Statler TS, Stern SA, Sunshine J, Weaver H, Wong I (2021) Lucy mission to the Trojan asteroids: science goals. *Planet Sci J* 2:171. <https://doi.org/10.3847/PSJ/abf840>
- Malin Space Science Systems (MSSS), Inc. (2013) ECAM Imaging System. <http://www.msss.com/brochures/ecam.pdf>
- Malin MC, Edgett K, Jensen E, Lipkaman L (2013) Mars Science Laboratory Project Software Interface Specification (SIS): Mast Camera (Mastcam), Mars Hand Lens Imager (MAHLI), and Mars Descent Imager (MARDI) Experiment Data Record (EDR), Reduced Data Record (RDR), and PDS Data Products. Version 1.2, JPL D-75410, Online at http://pds-imaging.jpl.nasa.gov/data/msl/MSLMST_0001/DOCUMENT/MSL_MMM_EDR_RDR_DPSIS.PDF
- Marchi S, Bell JF III, Bierhaus B, Spencer J (2023) Surface geology of Jupiter's Trojan asteroids. *Space Sci Rev* 219:44. <https://doi.org/10.1007/s11214-023-00985-9>
- Mottola S, Britt D, Brown ME, Buie MW, Noll K, Pätzold M (2024) Shapes, rotations, photometric and internal properties of Jupiter Trojans. *Space Sci Rev* 220
- Olkin CB, Levison H, Vincent M, Andrews J, Gray S, Good P, Noll K, Marchi S, Christensen P, Reuter D, Weaver H, Pätzold M, Bell JF III, Hamilton V, Dello Russo N, Simon A, Beasley M, Grundy W, Howett C, Spencer J, Ravine M, Caplinger M (2021) Lucy Mission to the Trojan Asteroids: Concept of Operations and Instrumentation. *Planet Sci J* 2:172. <https://doi.org/10.3847/PSJ/abf83f>
- ON Semiconductor (2017) MT9P0311/2.5-Inch 5 Mp CMOS Digital Image Sensor. Data Sheet online at <https://www.onsemi.com/pdf/datasheet/mt9p031-d.pdf>
- Pelgrift JY, Sahr EM, Nelson DS, Jackman CD, Benhacine L, Bos BJ et al (2018) In-flight calibration of the OSIRIS-REx optical navigation imagers. In: 1st annual RPI workshop on image-based modeling and navigation for space applications. Troy, New York
- Preusker F, Scholten F, Knollenberg J, Kührt E, Matz K-D, Mottola S, Roatsch T, Thomas N (2012) The northern hemisphere of asteroid (21) Lutetia—topography and orthoimages from Rosetta OSIRIS NAC image data. *Planet Space Sci* 66:54–63. <https://doi.org/10.1016/j.pss.2012.01.008>
- Ravine MA, Schaffner JA, Caplinger MA (2016) ECAM: a modular spaceflight imaging system – first flight deliveries. In: 3rd international workshop on instrumentation for planetary. #4106
- Sierks H, Lamy P, Barbieri C, Koschny D, Rickman H, Rodrigo R, A'Hearn MF, Angrilli F, Barucci MA, Bertaux J-L, Bertini I, Besse S, Carry B, Cremonese G, Da Deppo V, Davidsson B, Debei S, De Cecco M, De Leon J, Ferri F, Fornasier S, Fulle M, Hviid SF, Gaskell RW, Groussin O, Gutierrez P, Ip W, Jorda L, Kaasalainen M, Keller HU, Knollenberg J, Kramm R, Kührt E, Küppers M, Lara L, Lazzarin M, Leyrat C, Lopez Moreno JJ, Magrin S, Marchi S, Marzari F, Massironi M, Michalik H, Moissl R, Naletto G, Preusker F, Sabau L, Sabolo W, Scholten F, Snodgrass C, Thomas N, Tubiana C, Vernazza P, Vincent J-B, Wenzel K-P, Andert T, Pätzold M, Weiss BP (2011) Images of asteroid 21 lutetia: a remnant planetesimal from the early solar system. *Science* 334:487–490. <https://doi.org/10.1126/science.1207325>
- Spencer J et al (2023) The first Lucy Earth flyby (EGA1). *Space Sci Rev* 219. <https://doi.org/10.1007/s11214-023-01034-1>
- Zhao Y, Bell JF III et al (2024) Pre-flight and in-flight calibration and performance of the Terminal Tracking Cameras (TTCams) on the NASA Lucy Mission. *Space Sci Rev* 220